

Figure S1 Diagrammatic illustration for analysis of key carbohydrate metabolism enzymes activity (A), antioxidant enzymes activity (B) and 4D-proteomics (C).

Figure S2 SDS-PAGE of total proteins extracted from the last fully expanded leaf of wild type (WT) and *Az34* barley under optimum and low temperature.

Figure S3 Subcellular localization of the differentially expressed proteins for the comparisons of WT-LT vs WT-OT, *Az34*-LT vs WT-LT, *Az34*-OT vs WT-OT, and *Az34*-LT vs *Az34*-OT. (A) Subcellular localization of the differentially expressed proteins in the comparison of WT-LT vs WT-OT; (B) Subcellular localization of the differentially expressed proteins in the comparison of *Az34*-LT vs WT-LT; (C) Subcellular localization of the differentially expressed proteins in the comparison of *Az34*-OT vs WT-OT; (D) Subcellular localization of the differentially expressed proteins in the comparison of *Az34*-LT vs *Az34*-OT. OT, optimum temperature; LT, low temperature.

Figure S4 GO terms of the differentially expressed proteins for the comparisons of WT-LT vs WT-OT, *Az34*-OT vs WT-OT, *Az34*-LT vs WT-LT and *Az34*-LT vs *Az34*-OT. (A) GO terms of the differentially expressed proteins for the comparison of WT-LT vs WT-OT; (B) GO terms of the differentially expressed proteins for the comparison of *Az34*-OT vs WT-OT; (C) GO terms of the differentially expressed proteins for the comparison of *Az34*-LT vs WT-LT; (D) GO terms of the differentially expressed proteins for the comparison of *Az34*-LT vs *Az34*-OT. OT, optimum temperature; LT, low temperature.

Figure S5 Functional enrichment cluster of the differentially expressed proteins for the comparisons of WT-LT vs WT-OT, *Az34*-LT vs WT-LT, *Az34*-OT vs WT-OT, and *Az34*-LT vs *Az34*-OT. OT, optimum temperature; LT, low temperature.

Figure S6 Activities of key carbohydrate metabolism enzymes in the last fully expanded leaf of wild

type (WT) and *Az34* barley under optimum and low temperature. Ald, aldolase; UGPase, UDP-glucose pyrophosphorylase; Susy, sucrose synthase; AGPase, ADP-glucose pyrophosphorylase; HXK, hexokinase; PGI, phosphoglucomutase; G6PDH, glucose-6-phosphate dehydrogenase; PFK, phosphofructokinase; PGM, phosphoglucomutase; FK, fructokinase; vacInv, vacuolar invertase; cytInv, cytoplasmic invertase; cwInv, cell wall invertase. Different small letters indicate significant differences at  $P < 0.05$  level. Data are expressed as means  $\pm$  SEM ( $n=3$ ).

Figure S7 Activities of antioxidant enzymes in the last fully expanded leaf of wild type (WT) and *Az34* barley under optimum and low temperature. SOD, superoxide dismutase; CAT, catalase; APX, ascorbate peroxidase; POX, cytoplasmic peroxidase; cwPOX, apoplastic peroxidase; GST, glutathione S-transferase; MDHAR, monodehydroascorbate reductase; GR, glutathione reductase; DHAR, dehydroascorbate reductase. Different small letters indicate significant differences at  $P < 0.05$  level. Data are expressed as means  $\pm$  SEM ( $n=3$ ).

Figure S8 Concentrations of soluble sugar (A), soluble protein (B), proline (C) and  $H_2O_2$  (D) in the last fully expanded leaf of wild type and *Az34* barley under optimum temperature and low temperature. OT: optimum temperature, LT: low temperature. Different small letters indicate significant differences at  $P < 0.05$  level. Data are expressed as means  $\pm$  SEM ( $n=3$ ).

Figure S9 Biplot of principal component analysis (PCA) of ABA with physiological traits and ABA with enzyme activities performed separately in WT and *Az34* plants under optimum temperature and low temperature. (A) Biplot of PCA of ABA with physiological traits in WT and *Az34* plants under optimum temperature and low temperature; (B) Biplot of PCA of ABA with enzyme activities performed separately in WT and *Az34* plants under optimum temperature and low temperature. ABA, abscisic acid; *An*, net photosynthetic rate;  $g_s$ , stomatal conductance;  $\phi P_O$ , maximum quantum yield

for primary photochemistry;  $\psi_{EO}$ , probability that an electron moves further than  $Q_A$ ;  $\phi_{EO}$ , quantum yield for electron transport;  $\phi_{RO}$ , quantum yield for reduction of end electron acceptors at the PSI acceptor side.  $F_V/F_M$ , maximum quantum efficiency of photosystem II; AGPase, ADP-glucose pyrophosphorylase; UGPase, UDP-glucose pyrophosphorylase; FK, fructokinase; vacInv, vacuolar invertase; cytInv, cytoplasmic invertase; cwInv, cell wall invertase; SOD, superoxide dismutase; MDHAR, monodehydroascorbate reductase.

Figure S1

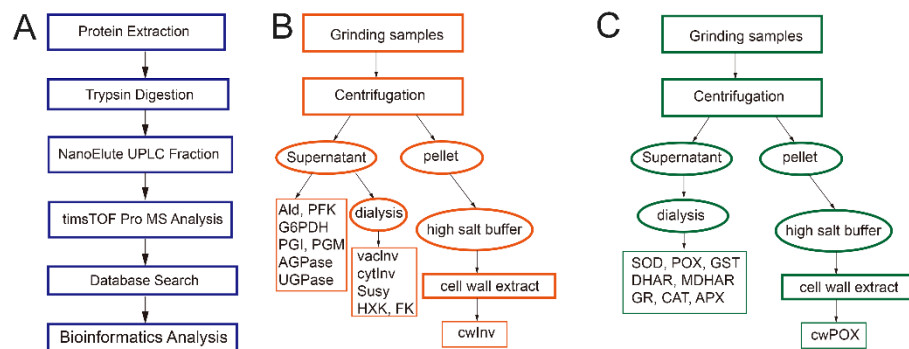


Figure S2

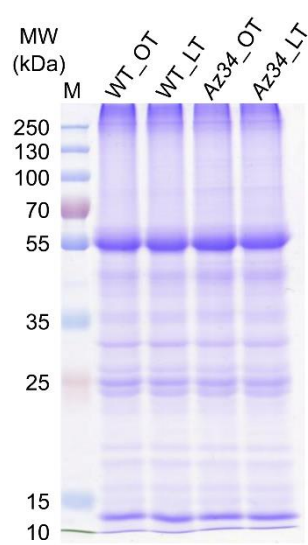


Figure S3

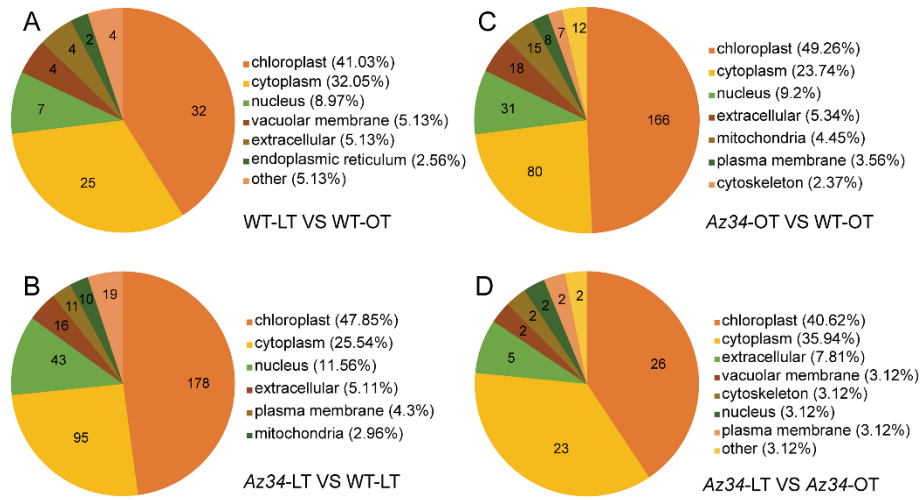
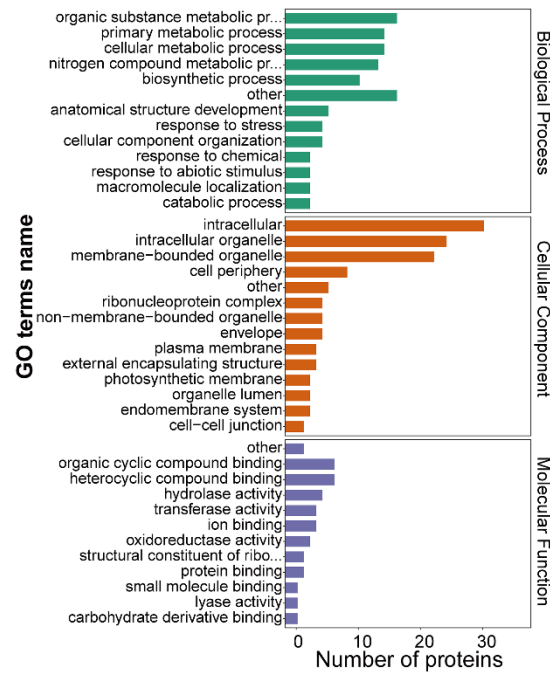
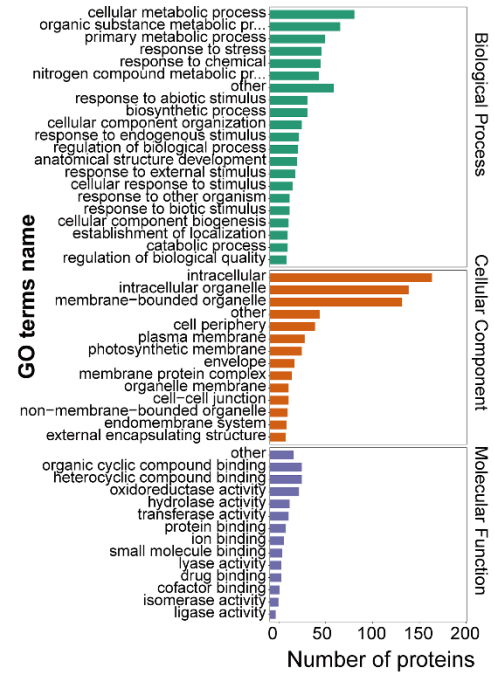


Figure S4

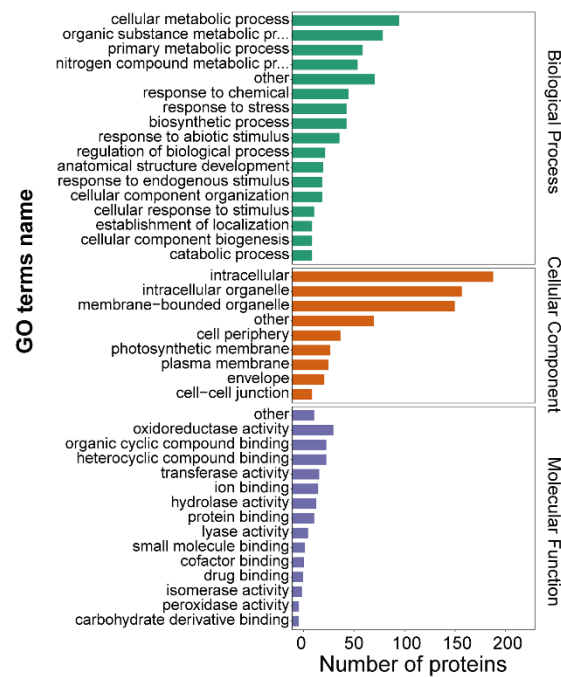
**A WT-LT vs WT-OT**



**B Az34-OT vs WT-OT**



**C Az34-LT vs WT-LT**



**D Az34-LT vs Az34-OT**

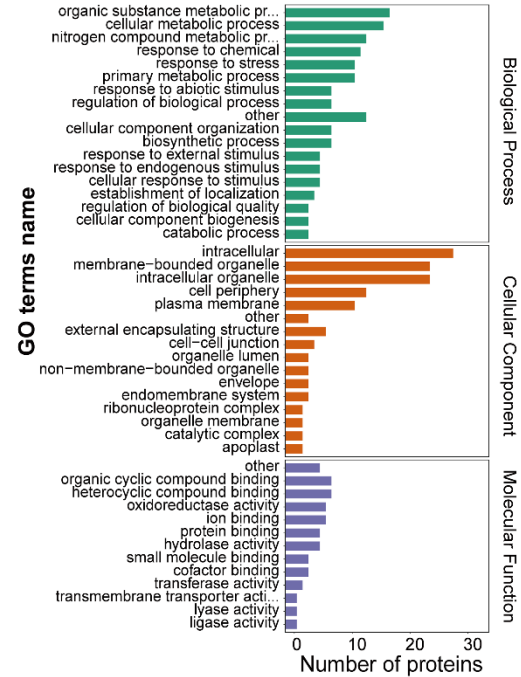


Figure S5





Figure S6

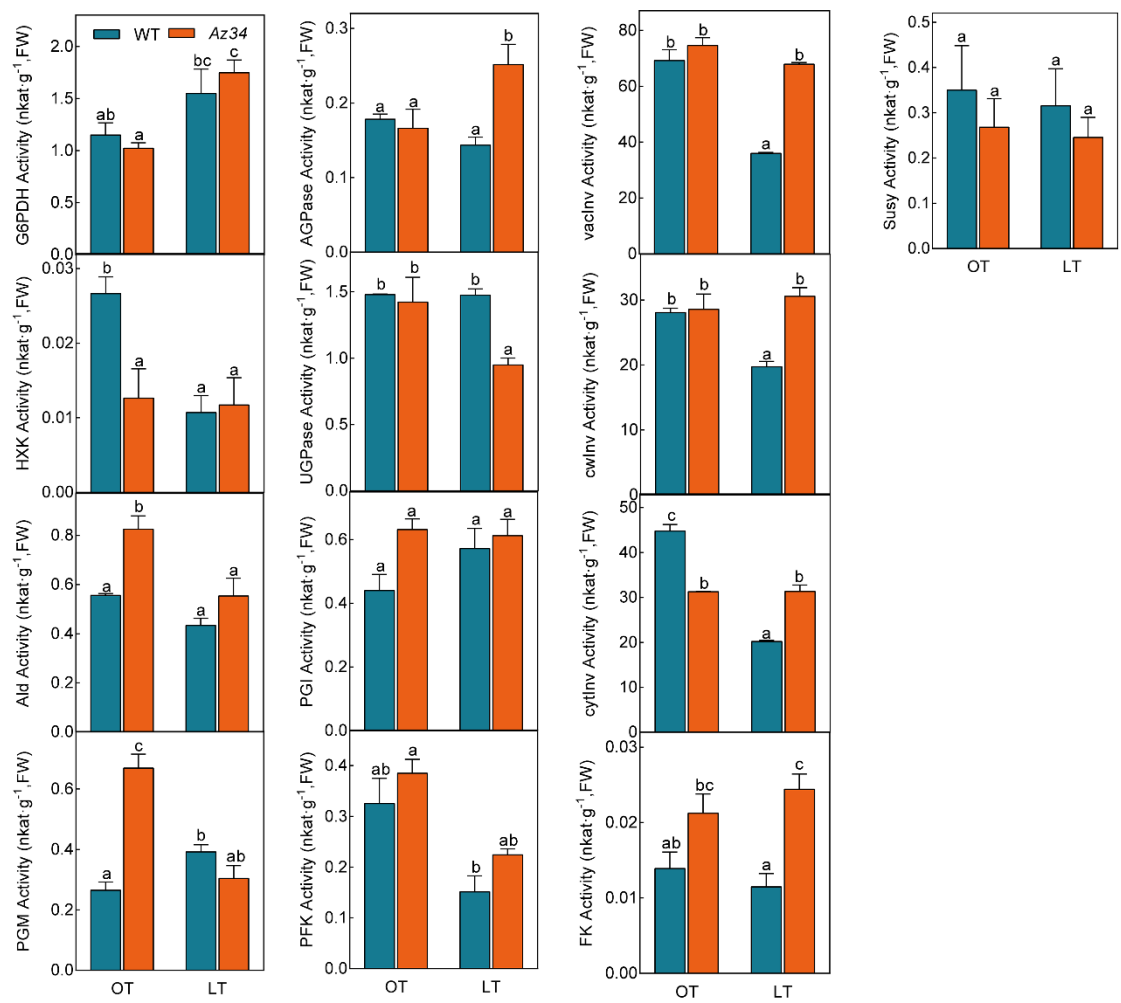


Figure S7

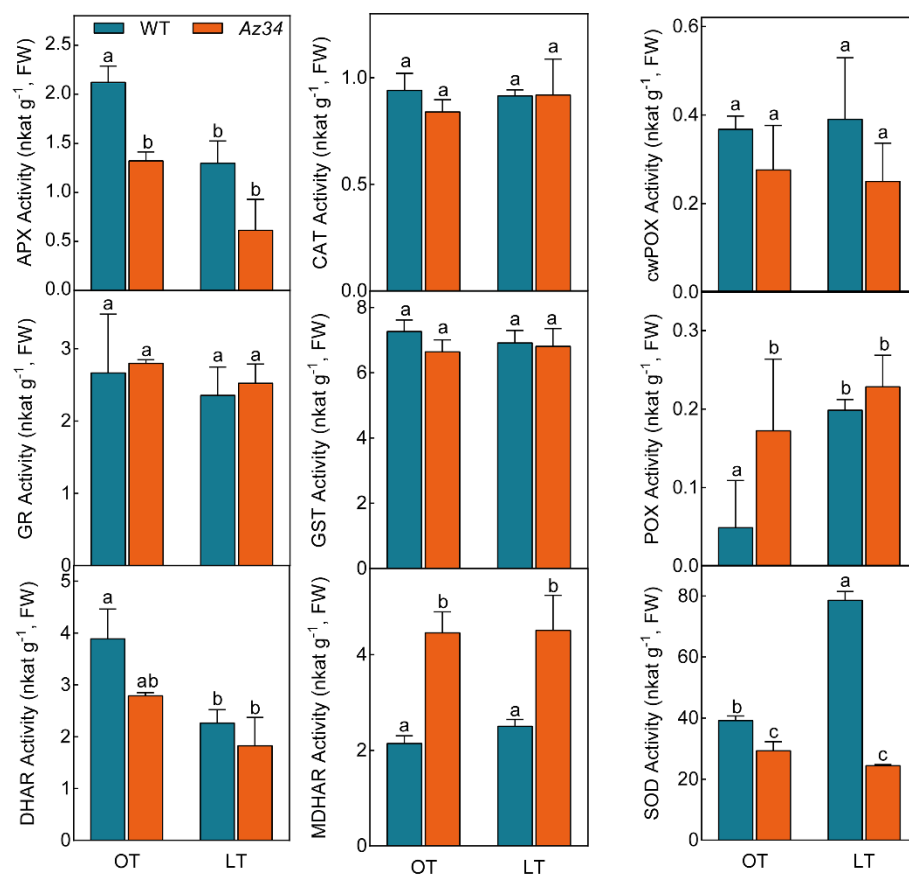


Figure S8

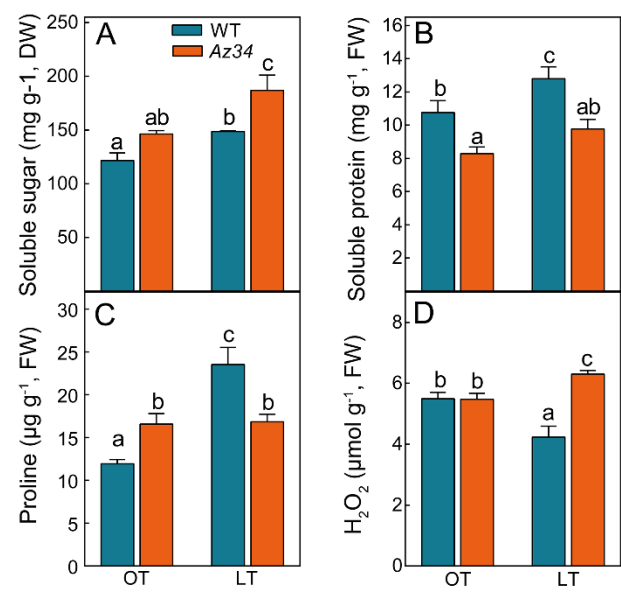


Figure S9

